Noise in Genetic Toggle Switch Models

M. Andrecut* and S. A. Kauffman

Institute for Biocomplexity and Informatics, University of Calgary,
2500 University Drive NW, Calgary, Alberta, T2N 1N4, Canada

Summary

In this paper we study the intrinsic noise effect on the switching behavior of a simple genetic circuit corresponding to the genetic toggle switch model. The numerical results obtained from a noisy mean-field model are compared to those obtained from the stochastic Gillespie simulation of the corresponding system of chemical reactions. Our results show that by using a two step reaction approach for modeling the transcription and translation processes one can make the system to lock in one of the steady states for exponentially long times.

1 Introduction

A large number of experimental data have demonstrated the presence of noise in gene regulation processes, where the small number of interacting molecules can lead to significant noise levels [1]-[3]. Obviously, the differential equations derived in a simplified mean-field model are deterministic and they fail to predict the fluctuations in the levels of molecular species presented in the system. Therefore, the mean-field description, which treats concentrations as continuous variables, is not suitable for systems consisting of small numbers of molecules in which individual reaction events dominate the behavior. In this case, stochastic kinetics methods are necessary for proper description of the system. A first possibility is to incorporate noise in the mean-field model by explicitly adding a random variable to the differential equations describing the system [4]-[6]. This approach results in a stochastic differential equation or Langevin equation. It is well known that the Langevin equation is asymptotically equivalent (under certain conditions) to the chemical master equation [7]. A second possibility is to employ a stochastic simulation algorithm for the chemical master equation. For example, the solutions of the stochastic formulation of coupled chemical reactions can be computed using the Monte Carlo algorithm introduced by Gillespie [8]. The Gillespie algorithm calculates the time evolution of the system by determining the probabilities of each discrete chemical reaction and the resulting changes in the number of each molecular species presented in the system. This algorithm has rigorous theoretical foundations, and gives the exact solution for a system of elementary chemical reactions in the approximation of a well-mixed environment. Also, the Gillespie algorithm accounts for most of the intrinsic noise of the system but not for the extrinsic noise generated by the intercellular interactions.

In this paper we study the intrinsic noise effect on the switching behavior of a simple genetic circuit corresponding to the genetic toggle switch model [9]. Such a genetic toggle switch can be formed from a pair of genes A and B that mutually repress each other's expression. We

*Corresponding author (email: mandrecu@ucalgary.ca).

consider two cases: a noisy mean-field approximation and Gillespie stochastic simulation. We show that the simplified mean-field model depends only on two parameters. These parameters measure the net effect of the expression, binding and degradation reaction rates. In a well-mixed system with a high number of molecules the reaction rates are considered constant. However, in reality the reaction rates fluctuates around some average values. For example, molecules fluctuate through structural microstates that can affect rate constants. Also, the cell is not a well stirred system, so local fluctuations in parameters such as pH can affect reaction constant rates. Assuming that the intrinsic noise arises from these processes, we add to each of these two parameters a random variable governed by a Gaussian distribution. This is a drastic approximation, because to be realistic one would need to model noise at each step of the expression, binding and degradation steps. However, this approach gives a simple alternative to capture the global contribution of these processes, to the intrinsic noise. The results obtained from the noisy mean-field model are compared to those obtained from the stochastic Gillespie simulation of the corresponding system of chemical reactions.

The paper is organized as following. In the first section we formulate the system of chemical reactions corresponding to the genetic toggle switch. The second section describes the mean-field model. In the third and forth sections we give the simulation results obtained from the noisy mean-field model and from the Gillespie stochastic simulation. In order to characterize the noise effects we compute the distributions of the switching time as a function of different parameters in the system and we show that the switching time is exponentially distributed. Also, we show that the constant rate of the protein degradation reactions and the total number of the molecules in the system play an important role in increasing the bistability of the system. We would like to note that the proposed noisy mean-field model captures very well most of the characteristics of the system, observed using the Gillespie stochastic simulation approach. Also, our simulations show that by using a two step reaction approach for modeling the transcription and translation processes one can make the system to lock in one of the steady states for extremely long times. These results provide a quantitative support to some conjectures previously reported in the literature.

2 The chemical system

Before describing the toggle switch system, let us analyze the gene expression process [10]. The genetic information is first transcribed into messenger RNA ($mRNA$) and then translated into proteins (M) by ribosomes ($Ribo$). The transcription process can be described by a sequence of reactions, in which the RNA polymerase ($RNAp$) binds to a promoter (P) leading to transcription of a complete $mRNA$ molecule:

$$RNAp + P \xrightarrow{k_1} C_1 \xrightarrow{k_2} ... \xrightarrow{k_n} C_n \xrightarrow{k_{n+1}} RNAp + P + mRNA. \quad (1)$$

Here, C_i corresponds to the complex formed in the intermediate reaction $i = 1, ..., n$. Since, the waiting times are independent statistical quantities, the waiting time for the whole sequence of intermediate complex formation is the sum of the waiting times for the individual steps. Also, we should note that the central limit theorem indicates that the lumped reaction of the open complex formation will tend to have a Gaussian distribution of waiting times, converging to a δ function for a very large number of intermediate steps. Thus, in terms of reaction rates (which

have units of inverse time) we have $k^{-1} = \sum_{i=1}^{n} k_i^{-1}$. For example, if we consider equal waiting times for each individual step, then from the above equation we obtain $k_i = nk$, $i = 1, ..., n$.

From the above considerations, it follows that the whole sequence of reactions (1) can be approximated by the following two reactions

$$RNAp + P \xrightarrow{k_\alpha} C \xrightarrow{k_\beta} RNAp + P + mRNA, \tag{2}$$

where $k_\alpha = \left(\sum_{i=1}^{n} \frac{1}{k_i}\right)^{-1}$ and $k_\beta = k_{n+1}$.

Let us now analyze the translation process, in which the information initially transcribed into $mRNA$ is now translated into r copies of proteins M. To describe this we consider the following additional reactions:

$$Ribo + mRNA \xrightarrow{k_\gamma} Ribo + mRNA + rM, \tag{3}$$

$$mRNA \xrightarrow{k_\delta} \emptyset. \tag{4}$$

The reaction (3) idealizes the multistep translation process, under the further idealization that if multiple ribosomes bind the $mRNA$ at a time, then a time averaged rate, r, of proteins can be used. The reaction (4) captures the degradation of $mRNA$. In a steady state $(dC/dt = 0)$, the rate of transcription is k_α and it balances the rate of degradation k_δ. Therefore, the mean number of $mRNA$ is $k_\alpha k_\delta^{-1}$. Each $mRNA$ produces r protein molecules at a rate k_γ, hence the overall rate of protein production is $rk_\alpha k_\gamma k_\delta^{-1}$.

From the above analysis it follows that the transcription and translation processes can be condensed in two reactions

$$RNAp + P \xrightarrow{k'} C \xrightarrow{k''} RNAp + P + M, \tag{5}$$

where $k' = rk_\alpha k_\gamma k_\delta^{-1}$ and $k'' = k_\beta$.

We conclude that this is the minimal system which takes into account the delay $\tau_\alpha \sim k_\alpha^{-1}$, corresponding to intermediate complex formation. Also, we should note that this analysis idealizes $mRNA$ and protein levels as their steady state levels.

A genetic toggle switch can be formed from a pair of genes A and B that mutually repress each other's expression. In this system protein homo-multimers are responsible for gene regulation and are allowed to bind to the promoter site. The chemical reactions are:

$$RNAp + P_A \xrightarrow{k'_A} C_A \xrightarrow{k''_A} RNAp + P_A + M_A, \tag{6}$$

$$RNAp + P_B \xrightarrow{k'_B} C_A \xrightarrow{k''_B} RNAp + P_B + M_B, \tag{7}$$

$$P_A + (M_B)_m \underset{k_A^0}{\overset{k_A^1}{\rightleftarrows}} P_A(M_B)_m, \tag{8}$$

$$P_B + (M_A)_n \underset{k_B^0}{\overset{k_B^1}{\rightleftarrows}} P_B(M_A)_n, \tag{9}$$

$$nM_A \underset{k_A^+}{\overset{k_A^-}{\rightleftarrows}} (M_A)_n, \tag{10}$$

$$mM_B \underset{k_B^+}{\overset{k_B^-}{\rightleftarrows}} (M_B)_m, \tag{11}$$

$$M_A \xrightarrow{k_A^\delta} \emptyset, \tag{12}$$

$$M_B \xrightarrow{k_B^\delta} \emptyset. \tag{13}$$

Eqs. (6)-(7) correspond to the gene expression process. Repression of gene expressions is captured in Eqs. (8)-(9). For example, gene A is expressed if and only if $(M_B)_m$ is not bound. Eqs. (10)-(11) corresponds to the multimerization reactions. Eqs. (12)-(13) take into account the degradation of the protein monomers.

3 The mean-field model

In this model we are simplifying gene expression even more by condensing the two reactions process (5) in only one reaction. This simplification can be made under the assumption that one of the two reactions is much slower/faster than the other one ($k' \gg k''$ or viceversa). Therefore, in the mean-field model we replace the first two equations (6)-(7) by

$$RNAp + P_A \xrightarrow{k_A} RNAp + P_A + M_A, \tag{14}$$
$$RNAp + P_B \xrightarrow{k_B} RNAp + P_B + M_B. \tag{15}$$

In a steady state the binding (8)-(9) and multimerisation reactions (10)-(11) are in equilibrium and we can write:

$$\begin{aligned} k_A^0[P_A][(M_B)_m] &= k_A^1[P_A(M_B)_m], & (16)\\ k_B^0[P_B][(M_A)_n] &= k_B^1[P_B(M_A)_n], & (17)\\ k_A^+[M_A]^n &= k_A^-[(M_A)_n], & (18)\\ k_B^+[M_B]^m &= k_B^-[(M_B)_m]. & (19) \end{aligned}$$

Therefore, the probabilities of the genes promoter states $\{P_A, P_A(M_B)_m\}$, $\{P_B, P_B(M_A)_n\}$ are in the ratio:

$$\begin{aligned} \frac{[P_A(M_B)_m]}{[P_A]} &= \frac{k_A^0}{k_A^1}[(M_B)_m] = \frac{k_A^0 k_B^+}{k_A^1 k_B^-}[M_B]^m = x_B^m, & (20)\\ \frac{[P_B(M_A)_n]}{[P_B]} &= \frac{k_B^0}{k_B^1}[(M_A)_n] = \frac{k_B^0 k_A^+}{k_B^1 k_A^-}[M_A]^n = x_A^n, & (21) \end{aligned}$$

where x_A and x_B are the reduced concentrations of the proteins. The probability of the promoter A/B to be in the state where the gene A/B is expressed is therefore:

$$\begin{aligned} f_A(x_A, x_B) &= \frac{1}{1+x_B^m}, & (22)\\ f_B(x_A, x_B) &= \frac{1}{1+x_A^n}. & (23) \end{aligned}$$

In a steady state, the rate of expression $k_{A/B}$ should be equal to the rate of degradation and we can write:

$$\begin{aligned} k_A f_A(x_A, x_B) &= k_A^\delta[M_A], & (24)\\ k_B f_B(x_A, x_B) &= k_B^\delta[M_B]. & (25) \end{aligned}$$

Thus, using the reduced concentrations we obtain the following steady state equations:

$$\begin{aligned} \eta_A f_A(x_A, x_B) &= x_A, & (26)\\ \eta_B f_B(x_A, x_B) &= x_B, & (27) \end{aligned}$$

where the coefficients

$$\eta_A = \frac{k_A}{k_A^\delta}\left(\frac{k_B^0 k_A^+}{k_B^1 k_A^-}\right)^{1/n}, \tag{28}$$

$$\eta_B = \frac{k_B}{k_B^\delta}\left(\frac{k_A^0 k_B^+}{k_A^1 k_B^-}\right)^{1/m}, \tag{29}$$

measure the net effect of the expression, binding and degradation rates.

It follows that around the steady state, the dynamics of the chemical system can be approximated by the following nonlinear dynamical system:

$$\frac{d}{dt}x_A = \eta_A f_A(x_A, x_B) - x_A = F_A(x_A, x_B), \tag{30}$$

$$\frac{d}{dt}x_B = \eta_B f_B(x_A, x_B) - x_B = F_B(x_A, x_B). \tag{31}$$

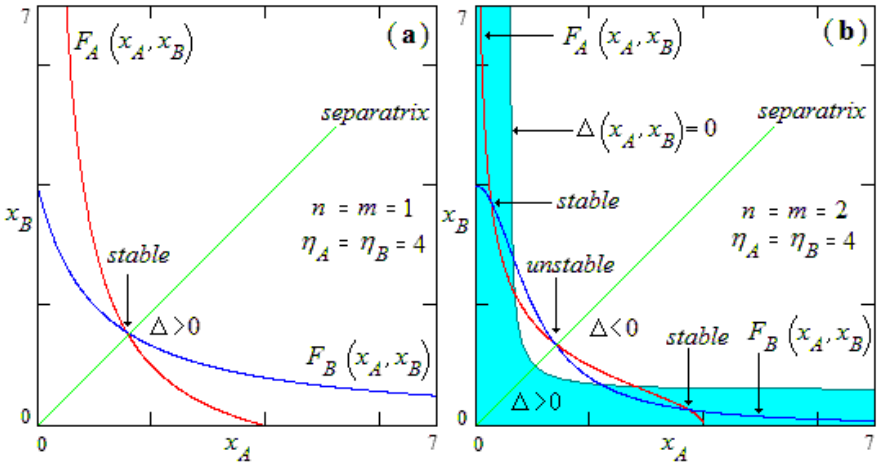

Figure 1: Geometrical structure of the mean-field model of the genetic toggle switch: (a) the monomer case; (b) the multimer case.

3.1 The monomer case

In this case we have $n = m = 1$. The intersection of the nullclines

$$F_A(x_A, x_B) = 0, \tag{32}$$

$$F_B(x_A, x_B) = 0, \tag{33}$$

gives the unique steady state of the dynamical system (Fig. 1a). In order to analyze the behavior of the above system we have to verify if this steady state is unstable.

A steady state can be classified into one of several classes using linear stability analysis. The stability matrix of the system is:

$$A(x_A, x_B) = \begin{pmatrix} \frac{\partial F_A}{\partial x_A} & \frac{\partial F_A}{\partial xB} \\ \frac{\partial F_B}{\partial x_A} & \frac{\partial F_B}{\partial x_B} \end{pmatrix}. \tag{34}$$

The analysis of the eigenvalues of $A(x_A, x_B)$ characterizes the type of steady state. To find the eigenvalues of A we need to solve the equation

$$|A - \lambda I| = 0, \tag{35}$$

which in this case gives the solutions:

$$\lambda_{1,2}(x_A, x_B) = -1 \pm \frac{\sqrt{\eta_A \eta_B}}{(1 + x_A)(1 + x_B)}. \tag{36}$$

At the steady state, the constants η_A and η_B can be eliminated from the Eqs. (26)-(27) and we obtain:

$$\lambda_{1,2}(x_A, x_B) = -1 \pm \sqrt{\frac{x_A x_B}{(1 + x_A)(1 + x_B)}} < 0, \quad \forall x_A, x_B > 0. \tag{37}$$

Obviously, the unique steady state is stable and the mean field model of the monomer system does not predict a switching behavior, which requires transitions between two steady states. Fig. 2 shows the typical dynamics of the system for different initial values and parameter values. One can see that the system converges quickly to the unique steady state. However, we will see later that by using the stochastic simulation approach, the system does exhibit switching behavior due to the intrinsic noise generated by the system.

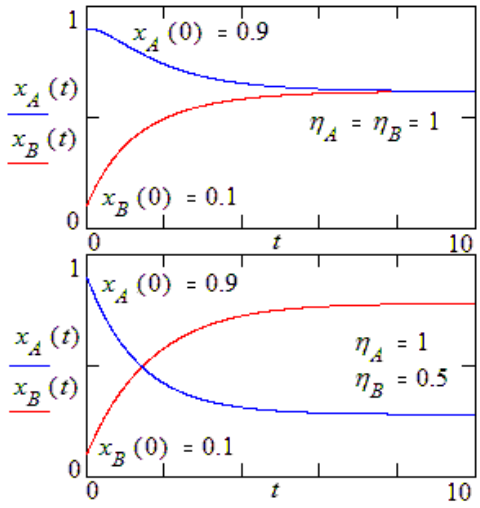

Figure 2: Dynamics of the mean-field model in the monomer case.

3.2 The multimer case

In this case, we have $n, m \geq 2$. The eigenvalues of the stability matrix are:

$$\lambda_{1,2}(x_A, x_B) = -1 \pm \sqrt{\frac{nm x_A^n x_B^m}{(1 + x_A^n)(1 + x_B^m)}}. \tag{38}$$

Therefore, the determinant of the stability matrix is given by:

$$D(x_A, x_B) = \lambda_1(x_A, x_B)\lambda_2(x_A, x_B) = \frac{1 + x_A^n + x_B^m - (nm - 1)x_A^n x_B^m}{(1 + x_A^n)(1 + x_B^m)}. \tag{39}$$

The sign of $D(x_A, x_B)$ coincides with the sign of the function:

$$\Delta(x_A, x_B) = 1 + x_A^n + x_B^m - (nm-1)x_A^n x_B^m. \quad (40)$$

So, if $\Delta(x_A, x_B) < 0$ at a steady state, that steady state is unstable in one direction (saddle point) $(\lambda_1 > 0, \lambda_2 < 0)$. Moreover, for any (x_A, x_B) the function $\Delta(x_A, x_B)$ has a definite sign, independent of the values of (η_A, η_B). The region $\Delta(x_A, x_B) < 0$ contains all the possible unstable steady states. The regions of positive and negative signs are separated by $\Delta(x_A, x_B) = 0$ (Fig. 1b). It can be easily shown numerically that for $n, m \geq 2$ and appropriate values of (η_A, η_B) the nullclines (32)-(33) intersect in three points, corresponding to the three steady states of the system (Fig. 1b). Two of the steady states are in the stability region, where $\Delta > 0$, while one steady state is in the unstable region $\Delta < 0$ (Fig. 1b).

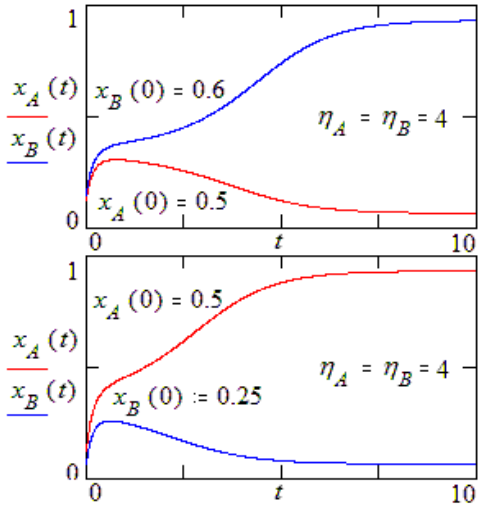

Figure 3: Dynamics of the mean-field model in the multimer case.

Fig. 3 shows the typical dynamics of the system for different initial values. One can see that, depending on the initial values, the system will settle in one of the stable states which are separated by the separatrix that travels through the unstable steady state. The separatrix divides the (x_A, x_B) state space into two basins of attraction. If $x_A(0) < x_B(0)$ then the system will settle in the upper steady state, while if $x_A(0) > x_B(0)$ then the system will settle in the lower upper state. The separatrix itself is a 1-dimensional manifold where trajectories flow to the unstable steady state.

We conclude that in order to obtain bistability, the protein inhibitors must repress the expression of the other with cooperativity greater than one. This suggests that repressor multimerization is necessary to obtain bistability. Higher-order multimerization will increase the robustness of the system, allowing weaker promoters to achieve bistability. The state of the toggle is switched by the application of a pulse that pushes the system away from the stable steady state, over the separatrix, and into the opposite basin of attraction.

4 Noisy mean-field model simulation

The system (30)-(31) is modified by assuming that the parameters $\eta_{A/B}$ are affected by noise $\eta_A = \eta_B = \eta_0 + \rho\xi$, where ξ is a random variable governed by a Gaussian distribution with zero

mean and variance equal to one, and $\rho \geq 0$ is a parameter measuring the strength (variance) of the noise. The system of differential equations is solved numerically using the 4th-order Runge-Kutta method. The Gaussian distribution was sampled by the use of the standard Box-Muller method. As a measure of flipping the switch from one state to the other we are considering $q(t) = x_A(t) - x_B(t)$ which serves as an order parameter. Below we give the numerical results obtained for the monomer and multimer systems.

4.1 The monomer case

In Fig. 4 we give the temporal evolution of $q(t)$. The parameter η is set to $\eta_0 = 2$ and the noise strength is $\rho = 0.5$. The initial state corresponds to the stable state of the deterministic system: $x_A(0) = 1$, $x_B(0) = 1$. Without the noise the system will stay in this stable state. If the noise is present then the system will fluctuate around the stable state. In Fig. 5 we give the distributions of the noise $h(\eta)$ and of the order parameter $h(q)$ for the above initial values. One can easily see that $h(q)$ is also Gaussian distributed. This is normal since the system has only one stable state from which it cannot escape.

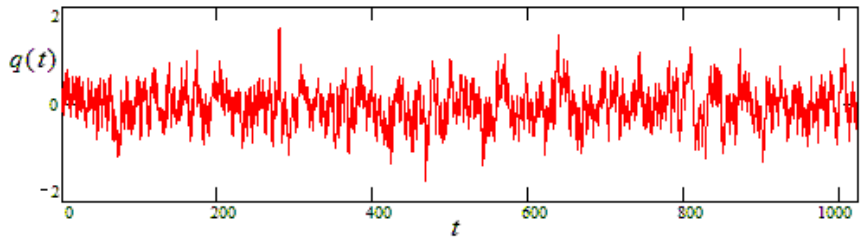

Figure 4: Temporal evolution of the order parameter $q(t)$ for the noisy mean-field model in the monomer case.

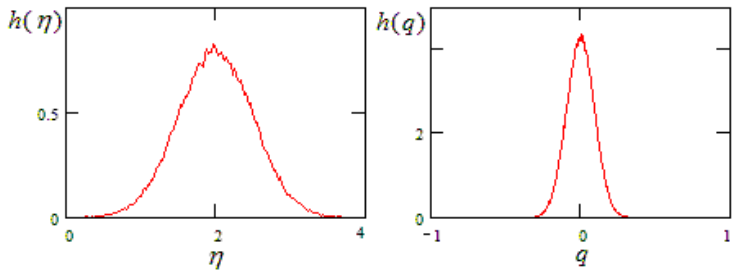

Figure 5: The distributions of the noise $h(\eta)$ and of the order parameter $h(q)$ for the noisy mean-field model in the monomer case.

Let us now consider the switching time parameter θ which is defined as the time interval for which the system stays above/below the separatrix. Assuming that the distribution is exponential

$$h(\theta) = c_1 \exp(-c_2 x), \tag{41}$$

then we obtain the cumulative distribution

$$H(x \geq \theta) = \int_\theta^\infty h(x)dx = \exp(a\theta + b), \tag{42}$$

where $a = -c_2$, $b = \ln(c_1/c_2)$. Therefore

$$\ln(H(\theta)) = a\theta + b, \tag{43}$$

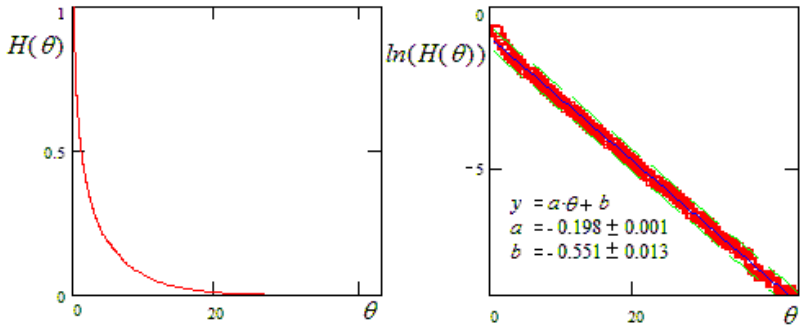

Figure 6: The fit of the cummulative distribution $H(\theta)$ of the switching time parameter θ for the noisy mean-field model in the monomer case.

and we should be able to fit the simulation results using a straight line. One can see that the fit results correspond almost perfectly to the exponential distribution (Fig. 6).

4.2 The multimer case

In our simulations we consider the dimer system with $n = m = 2$ and $\eta_A = \eta_B = \eta_0 = 2.2$. Also, we consider that the initial state of the system corresponds to the unstable state of the deterministic system (which is obtained solving the steady state equations). Without the noise, the system will stay in this unstable state situated on the separatrix. If the noise is present, then the state of the system will move above or below the separatrix. If the noise strength is low, then the system will be locked and it will fluctuate around the upper/lower steady state. If the noise strength is high enough then the state of the system can cross the separatrix and we obtain a switching behavior. In Fig. 7 we give the temporal evolution of the order parameter $q(t)$ for the following values of the noise strength is $\rho = 0.3, 0.4, 0.5$. One can see that by increasing the noise strength the stability of the system decreases and the switching behavior increases in intensity. In Fig. 8 we give the distributions of the noise $h(\eta)$ and respectively of the order parameter $h(q)$. One can see how the probability around the separatrix increases by increasing the noise strength parameter ρ. Also, the two probabilities maxima, corresponding to the stable states of the deterministic system, decrease as the noise strength increases. In Fig. 9 we give the fit of the cumulative distribution of the switching time parameter θ for the same values of the noise strength.

5 Stochastic simulation

Here we give a short description of the stochastic Gillespie algorithm. The rigorous derivation of the algorithm has been given elsewhere and it has been shown to remain ”exact” for arbitrary low number of molecules [8]. Consider a system composed of N chemical species X_ν $(\nu = 1, ..., N)$ interacting through M reactions R_μ $(\mu = 1, ..., M)$ in the cell volume V. Every reaction μ is characterized by its stochastic rate constant k_μ, which depends on the physical properties of the molecules taking part in the reaction. The product $k_\mu dt$ is the probability that one elementary reaction μ happens in the next infinitesimal time interval dt. For the above system of reactions, the algorithm answers the following questions: (a) what is the waiting time τ for the next reaction to occur and (b) which reaction μ in the system will occur. These questions

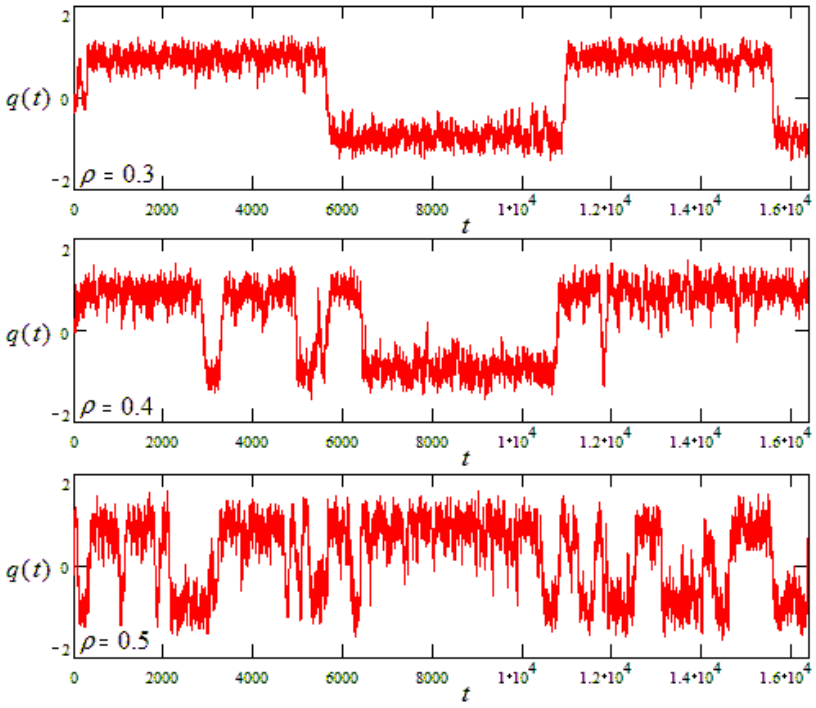

Figure 7: Temporal evolution of the order parameter $q(t)$ for the noisy mean-field model in the multimer case.

are answered by generating two random numbers according to the following probability density function:

$$P(\tau, \mu) = a_\mu \exp(-a_0 \tau), \tag{44}$$

where

$$a_\mu = m_\mu k_\mu, \quad a_0 = \sum_{\mu=1}^{M} a_\mu. \tag{45}$$

Here, m_μ is the number of distinct reactant combinations available for the reaction R_μ at the given state of the system. The coefficient a_μ is called the propensity of reaction R_μ. $P(\tau, \mu)$ is the probability that the next reaction will occur in the infinitesimal time interval $d\tau$ and that it will be the R_μ reaction. After determination of (τ, μ), the numbers of molecules in the system and the time of the simulation are adjusted accordingly. The larger the propensity is, the greater the chance that a given reaction will happen in the next step of the simulation. Also, we should mention that there is no constant timestep in the simulation. The timestep is determined in every iteration and it takes different values depending on the state of the system. The implementation of the algorithm is straightforward and the reader can find excellent descriptions in the literature [11]-[12].

5.1 The monomer case

This is the case of system (6)-(13) with $n = m = 1$ and in which the Eqs. (6)-(7) are replaced by Eqs. (14)-(15). In Fig. 10a we have a typical temporal evolution of the order parameter $q(t)$. All the reaction constants are set to one. The initial values of the molecule numbers are set to zero, with the exception of $RNAp = 200$ and $P_A = P_B = 1$. The behavior of the system depends very strongly on the degradation reaction constants. In Fig. 11 we give the distribution

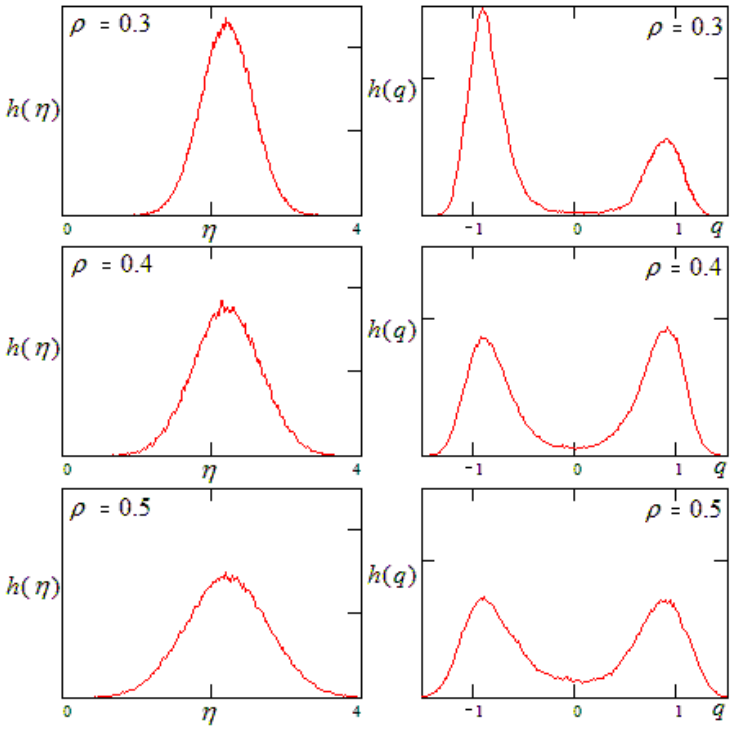

Figure 8: The distributions of the noise $h(\eta)$ and of the order parameter $h(q)$ for the noisy mean-field model in the multimer case.

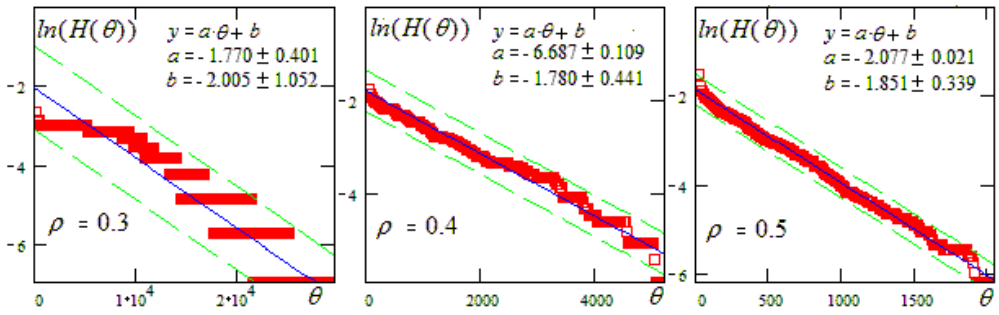

Figure 9: The fit of the cummulative distribution $H(\theta)$ of the switching time parameter θ for the noisy mean-field model in the multimer case.

of the order parameter $q(t) = M_A - M_B$ as a function of the degradation reaction constants $k_A^\delta = k_B^\delta = k^\delta$. One can see that by increasing the value of k^δ the distribution changes its aspect considerably. For small $k^\delta = 0.1$ (which is equivalent to $\eta_0 = 10$ in the noisy mean-field model) the distribution is close to the Gaussian distribution obtained in the noisy mean-field model (Fig. 5). However, by increasing the value to $k^\delta = 0.25; 0.5; 1$ (equivalent to $\eta_0 = 4; 2; 1$ in the noisy mean-field model) a bistable behavior emerges in the system. We should mention that this bistable behavior is actually not predicted by the mean-field model. This behavior occurs because the states $(x_A \to \infty, x_B \to 0)$ and $(x_A \to 0, x_B \to \infty)$ are also asymptotic solutions of the steady states equations (11). The stochastic system is attracted by these steady states, but because the number of protein molecules cannot increase to infinite (they are limited by the total number of molecules in the system) and because of the intrinsic noise, the system will tend to switch its state above/below the separatrix. Our simulations have shown that the system becomes more bistable by increasing the degradation reaction constants k^δ. However, the switching time cannot be made arbitrarily long. This means that the system cannot be

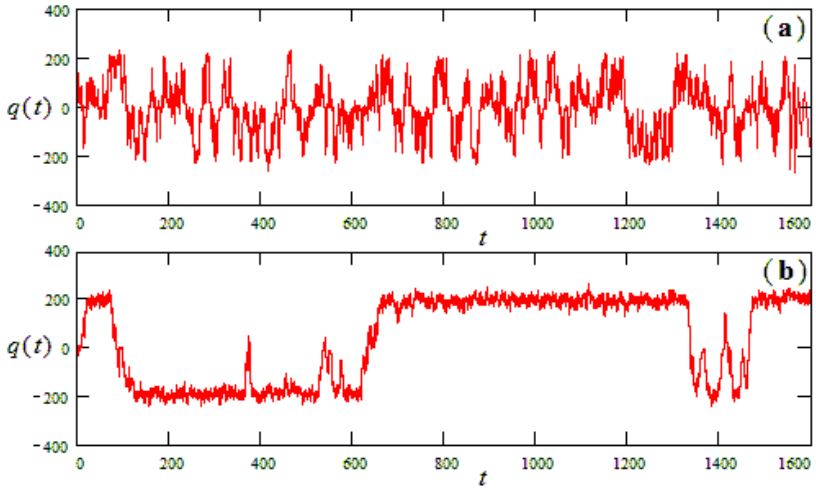

Figure 10: Temporal evolution of the order parameter $q(t)$ for the Gillespie stochastic simulation: (a) the monomer case; (b) the multimer case.

locked in a state above/below the separatrix for an arbitrary long period of time. In Fig. 13a-13b we give the fit of the cumulative distribution of the switching time parameter θ for a typical trajectory of the system ($k^{\delta} = 1$).

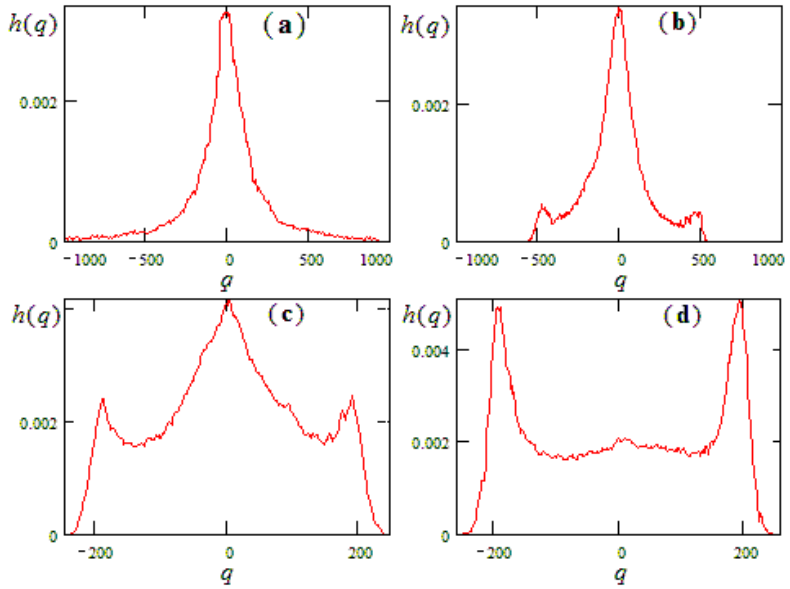

Figure 11: The distribution of the order parameter $h(q)$ for the Gillespie stochastic simulation as a function of the degradation constant in the monomer case: (a) $k^{\delta} = 0.1$; (b) $k^{\delta} = 0.25$; (c) $k^{\delta} = 0.5$; (d) $k^{\delta} = 1$.

5.2 The multimer case

Because the simulation process is quite intensive we are limiting our investigation to the dimer case in which $n = m = 2$. Also, first we assume that the Eqs. (6)-(7) are replaced by Eqs. (14)-(15). In Fig. 10b we have a typical temporal evolution of the order parameter $q(t)$. All the reaction constants are set to one with the exception of $k_{A/B} = 2.2$ and $k^{+}_{A/B} = k^{-}_{A/B} = 10^{-3}$. This means that the number of dimers in the system is kept at a low level. This also means

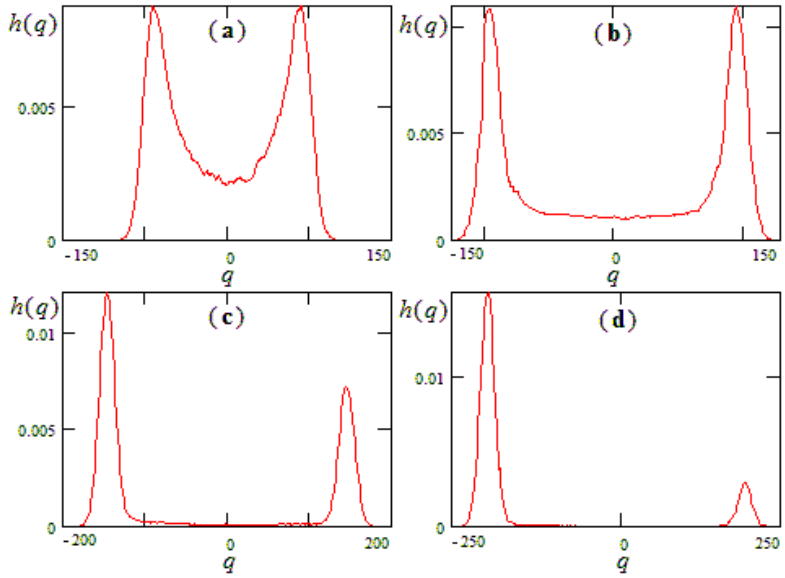

Figure 12: The distribution of the order parameter $h(q)$ for the Gillespie stochastic simulation as a function of the number of $RNAp$ molecules in the multimer case: (a) $N = 50$; (b) $N = 100$; (c) $N = 150$; (d) $N = 200$.

that the dimer creation is a much slower process compared to the other reactions. The effect of this is the increase in the bistability of the system. This values of the reaction constant rates will give an equivalent value of $\eta_0 = 2.2$, which we have used in the noisy mean-field simulation. The initial values of the molecule numbers are set to zero, with the exception of $RNAp = 200$ and $P_A = P_B = 1$. Our simulations have shown that the bistability of the switch increases very fast by increasing the number of molecules in the system. In Fig. 12 we have represented the distribution of the order parameter $q(t)$ as a function of the initial number of $RNAp$ molecules $(RNAp = 50; 100; 150; 200)$. The bistability of the system and the switching time increases very fast with the increase of the number of the $RNAp$ molecules. This gives a quantitative support to the conjecture that the switching time grows exponentially with the number of molecules from the system [13]. This conjecture is also sustained by the stochastic simulations reported in [14] for a different model. Also, we should note that the system can be locked for a long period of time around the upper/lower steady state by increasing the number of molecules in the system. In Fig. 13c-13d we give the fit of the cumulative distribution of the switching time parameter θ for a typical trajectory of the system ($RNAp = 100$). The distribution of the switching time is again exponential.

We have performed also simulations for the more general case of the system (6)-(13) in which we have considered the transcription and translation processes described by two reaction steps, with the assumption that one of the two reactions is much more slower/faster than the other one ($k' \gg k''$ or viceversa). For very small values of the ratio $k'/k'' \gg 10^{-2}$ (or viceversa) we recover similar results to those obtained by assuming only one reaction step. However, by using the same initial values as before and setting the ratio $k'/k'' \approx 10^{-2}$ (or viceversa) the system locks around one of the steady states for extremely long time. We have not counted any switching for extremely long trajectories (10^7 simulation steps). This corresponds to lifetimes measured in years. Such long lifetimes have been previously reported in the literature [15]. Our simulations give a quantitative support for these results.

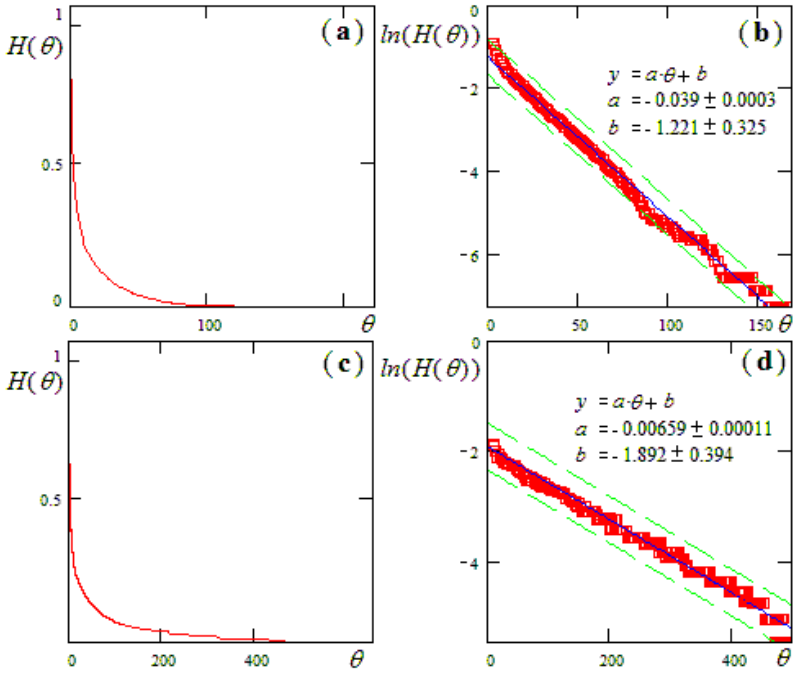

Figure 13: The fit of the cummulative distribution $H(\theta)$ of the switching time parameter θ for the Gillespie stochastic simulation: (a)-(b) the monomer case; (c)-(d) the multimer case.

Conclusion

In this paper we have proposed a noisy mean-field model of the genetic toggle switch. We have shown that this model approximates very well the characteristics of the system, observed using the Gillespie stochastic simulation algorithm. This means that the noisy mean field model captures very well the intrinsic noise effects corresponding to the considered stochastic system. In order to characterize the noise effects we have computed the distributions of the switching time as a function of different parameters in the system and we have shown that the switching time is exponentially distributed. We have shown that the constant rate of the protein degradation reactions and the total number of the molecules in the system play important roles in increasing the bistability of the system. Also, our simulations have shown that by using a two step reaction approach for modeling the transcription and translation processes one can make the system lock in one of the steady states for extremely long times. These results provide a quantitative support to some conjectures previously reported in the literature [13]-[15].

Acknowledgement

This research was supported by iCORE under Grant No. RT732223.

References

[1] I. L. Ross, C. M. Browne, D. A. Hume, Transcription of individual genes in eukaryotic cells occurs randomly and infrequently, *Immunology and Cell Biology,* 72, 177 (1994).

[2] E. M. Ozbundak, M. Thattai, I. Kurtser, A. D. Grossman, A. van Oudenaarden, Regulation of noise in the expression of a single gene, *Nature Genetics,* 31, 69 (2002).

[3] M. B. Elowitz, A. J. Levine, E. D. Siggia, P.S. Swain, Stochastic gene expression in a single cell, *Science,* 207, 1183 (2002).

[4] J. Hasty, J. Pradines, M. Dolnik, J. J. Collins, Noise-based switches and amplifiers for gene expression, *Proceedings of the National Academy of Sciences of the United States of America,* 97, 2075 (2000).

[5] T. B. Kepler, T. C. Elston, Stochasticity in Transcriptional Regulation: Origins, Consequences, and Mathematical Representations, *Biophysical Journal,* 81, 3116 (2001).

[6] T. Toulouse, P. Ao, I. Shmulevich, S. A. Kauffman, Noise in a Small Genetic Circuit that Undergoes Bifurcation *Complexity,* 11, 45 (2005).

[7] N. G. Van Kempen, Stochastic Processes in Physics and Chemistry (Elsevier Science, 2001).

[8] D. T. Gillespie, Exact stochastic simulation of coupled chemical reactions, *Journal of Physical Chemistry,* 81, 2340 (1977).

[9] T. S. Gardner, C. R. Cantor, J. J. Collins, Construction of a genetic toggle switch in Escherichia coli, *Nature,* 403, 339 (2000).

[10] H. H. McAdams, A. Arkin, Stochastic mechanisms in gene expression, *Proceedings of the National Academy of Sciences of the United States of America,* 94, 814 (1997).

[11] D. Adalsteinsson, D. McMillen, T. C. Elston, Biochemical Network Stochastic Simulator (BioNetS): software for stochastic modeling of biochemical networks, *BMC Bioinformatics,* 5, 24 (2004).

[12] A. Kierzek, STOCKS: STOChastic Kinetic Simulations of biochemical systems with Gillespie algorithm, *Bioinformatics,* 18, 3 (2002).

[13] W. Bialek, Physics arXiv (http://xxx.lanl.gov/), cond-mat/0005235.

[14] P. B. Warren, P. R. ten Wolde, Enhancement of the Stability of Genetic Switches by Overlapping Upstream Regulatory Domains, *Physical Review Letters,* 92, 128101 (2004).

[15] E. Aurell, S. Brown, J. Johanson, K. Sneppen, Stability puzzles in phage λ, *Physical Review E,* 65, 051914 (2002).